Available online at www.sciencedirect.com
ScienceDirect
Tetrahedron
Tetrahedron 63 (2007) 435–444

Shearinines D–K, new indole triterpenoids from an endophytic *Penicillium* sp. (strain HKI0459) with blocking activity on large-conductance calcium-activated potassium channels

Minjuan Xu,[a,b,e] Guido Gessner,[c] Ingrid Groth,[b] Corinna Lange,[b] Arnulf Christner,[b] Torsten Bruhn,[e] Zhiwei Deng,[d] Xiang Li,[a] Stefan H. Heinemann,[c] Susanne Grabley,[b] Gerhard Bringmann,[e] Isabel Sattler[b,*] and Wenhan Lin[a,*]

[a]*State Key Lab of Natural and Biomimetic Drugs, Peking University, Beijing 100083, PR China*
[b]*Leibniz Institute for Natural Products Research and Infection Biology, Hans-Knöll Institute, Beutenbergstr. 11a, D-07745 Jena, Germany*
[c]*Center for Molecular Biomedicine, Department of Biophysics, Friedrich Schiller University, Drackendorfer Str. 1, D-07743 Jena, Germany*
[d]*Analytical and Testing Center, Beijing Normal University, Beijing 100073, PR China*
[e]*Institute of Organic Chemistry, University Würzburg, Am Hubland, D-97074 Würzburg, Germany*

Received 11 September 2006; revised 16 October 2006; accepted 19 October 2006
Available online 14 November 2006

Abstract—A chemical examination of the endophytic fungus *Penicillium* sp. isolated from the mangrove plant *Aegiceras corniculatum* resulted in the isolation and characterization of eight new indole triterpenes named shearinines D–K (**1**–**8**), along with shearinine A (**9**), paspalitrem A (**10**), and paspaline (**11**). Their stereostructures were determined by extensive spectroscopic data analyses and quantum chemical circular dichroism calculations. The biosynthetic relationship of all 11 alkaloids is suggested. Shearinines D (**1**), E (**2**), and (with reduced potency) G (**4**) exhibit significant in vitro blocking activity on large-conductance calcium-activated potassium channels.

1. Introduction

Mangrove forests are distributed in most tropical and subtropical regions in the world, several mangrove species are a valuable source of useful metabolites for medicinal usage.[1] Some of the potency of mangrove plants may be due to mutualistic fungal endophytes associated with host plants, in fact fungi from mangroves are the second largest group among the marine fungi.[2] In general, the production of secondary metabolites that are potentially useful for pharmaceutical and agricultural applications is widespread among endophytic fungi.[3] One possible target of such mycotoxins is the large-conductance, calcium- and voltage-activated potassium (BK_{Ca}) channel, which is implicated in various diseases, including epilepsia, hypertension or erectile dysfunction.[4] Our previous investigation of endophytic microorganisms from mangrove plants resulted in a number of bioactive and structurally unique metabolites.[5–7] In the course of continuous investigations on natural products for drug oriented lead compound discovery and the metabolic relationship between mangrove plants and their endophytes, a fungus *Penicillium* sp. was isolated from the stems of *Aegiceras corniculatum* (Aegiceritaceae),[8] a mangrove plant from which seven new phenolic and quinone derivatives with anticancer activity were obtained.[9,10] From the acetone extract of mycelium yielded from a 200 L cultivation, 11 indole triterpenes (**1**–**11**) belonging to the janthitrem class were isolated. The known compounds shearinine A (**9**),[11] paspalitrem A (**10**),[12] and paspaline (**11**)[13] were identified on the basis of NMR data and by comparison of their spectroscopic data with those in literature. In this paper, we report the structural elucidation of the eight new indole triterpenes, shearinines D–K (**1**–**8**) (Fig. 1, Scheme 1). Finally, results from an activity study of the novel compounds on in vitro blocking activity on large-conductance calcium- and voltage-activated potassium (BK_{Ca}) channels are presented.

Keywords: Indole triterpenoids; Mangrove; *Penicillium* sp.; BK_{Ca} channels; Quantum chemical CD calculations; Circular dichroism.
* Corresponding authors. Tel.: +86 10 8280 6188; fax: +86 10 8280 2724 (W.L.); tel.: +49 3641 656920; fax: +49 3641 656922 (I.S.); e-mail addresses: isabel.sattler@hki-jena.de; whlin@bjmu.edu.cn

0040–4020/$ - see front matter © 2006 Elsevier Ltd. All rights reserved.
doi:10.1016/j.tet.2006.10.050

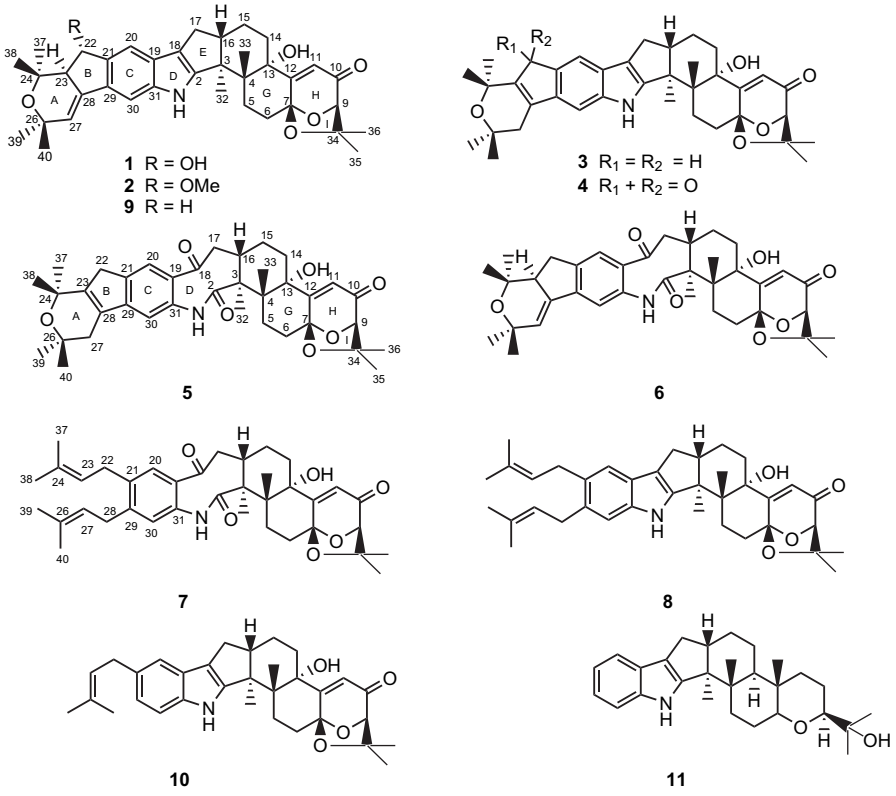

Figure 1. Chemical structures of shearinines D–K (**1**–**8**), shearinine A (**9**), paspalitrem A (**10**), and paspaline (**11**).

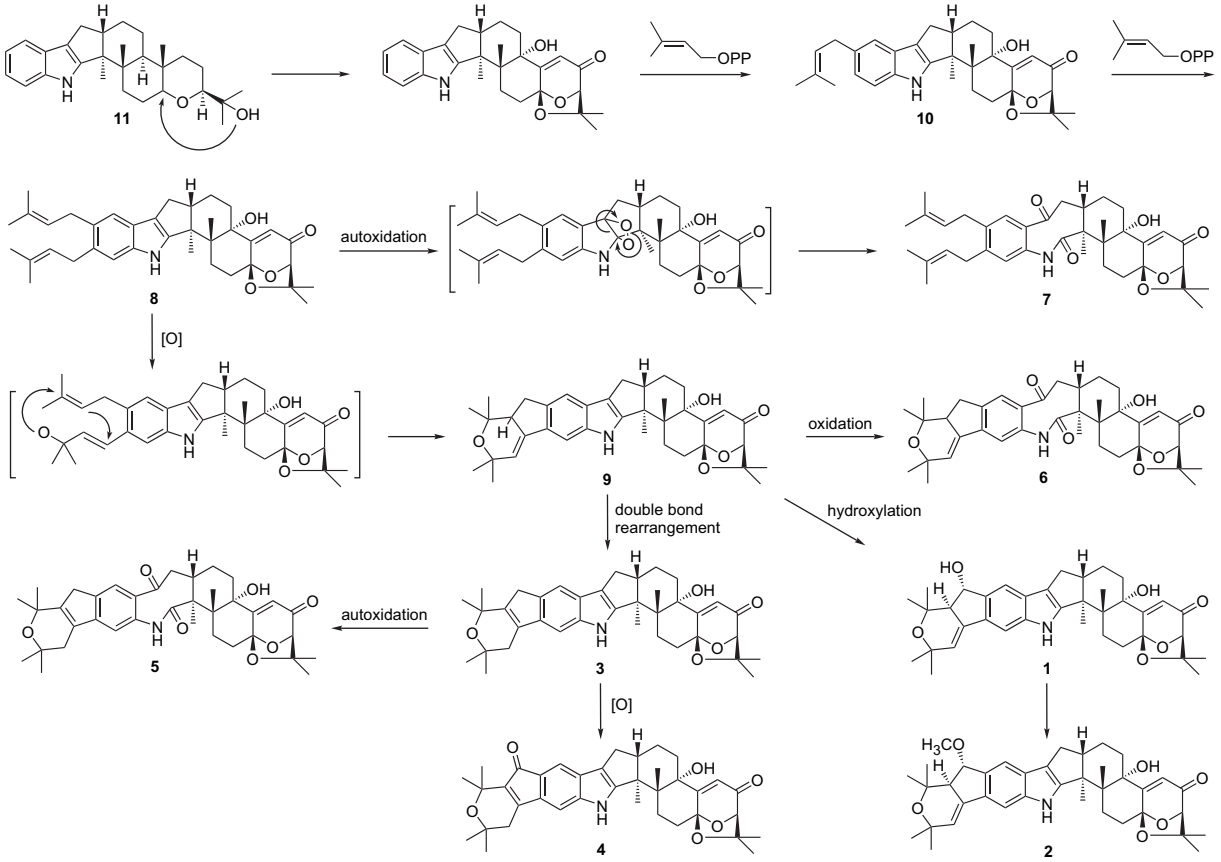

Scheme 1. Proposed biosynthetic pathway for shearinines A (**9**), D–K (**1**–**8**), paspalitrem A (**10**), and paspaline (**11**) in *Penicillium* sp. (HKI0459).

2. Results

2.1. Planar structures of shearinines D (1)–G (4)

The molecular formula of shearinine D (**1**) was determined to be $C_{37}H_{45}NO_6$ by HRESIMS (*m/z* 622.3163 $[M+Na]^+$, calcd 622.3139), indicating 16° of unsaturation and 16 amu more than that of shearinine A.[11] The IR absorptions at 3421 (br) and 1685 cm^{-1} suggested the presence of hydroxyl and carbonyl groups. The ^{13}C NMR and DEPT spectra displayed all 37 carbons, including eight methyls, five methylenes, and eight methines. Out of 16 quaternary carbons, signals at δ_C 169.6 (s, C-12) and 197.0 (s, C-10) implied the presence of an unsaturated keto group (Table 1). For the eight methyl groups, the ^1H NMR spectrum revealed eight aliphatic methyl singlets at δ_H 1.41 (s, H_3-32), 1.25 (s, H_3-33), 1.20 (s, H_3-35), 1.46 (s, H_3-36), 1.51 (s, H_3-37), 1.14 (s, H_3-38), 1.36 (s, H_3-39), and 1.37 (s, H_3-40) (Table 2). The six methines were consistent with two aromatic singlets at δ_H 7.50 (s, H-20) and 7.36 (s, H-30), two olefinic signals at δ_H 5.85 (s, H-11) and 5.98 (d, *J*=2.8 Hz, H-27), and two aliphatic protons at δ_H 2.69 (dd, *J*=2.8, 5.6 Hz, H-23) and 4.33 (s, H-9). The ^1H NMR spectrum also revealed the presence of a D_2O exchangeable proton at δ_H 7.75 (s) for an indole amine. The HMQC spectrum allowed to assign all protons to their corresponding carbon atoms. The ^1H and ^{13}C NMR data, in combination with the HMBC correlation analysis, resulted in the gross structure of **1**, which is closely related to that of shearinine A (**9**).[11] The main difference between **1** and the latter was found in ring B where the methylene signals of C-22 of shearinine A was replaced by those of an hydroxylated methine at δ_C 76.4 (d, C-22) and δ_H 4.98 (d, *J*=5.6 Hz, H-22) of **1**. The HMBC correlations between H-22 and C-24 (δ_C 73.8, s), C-28 (δ_C 138.6, s), C-29 (δ_C 131.8, s), and C-20 (δ_C 113.9, d) confirmed this substitution. Therefore, the structure of shearinine D (**1**) was determined as 22-hydroxy-shearinine A.

The HRFABMS of shearinine E (**2**) indicated its molecular formula to be $C_{38}H_{47}NO_6$ (*m/z* 613.3396, calcd 613.3397), and thus 14 amu more than that of **1**. The ^1H and ^{13}C NMR data of **2** were in close agreement with those of **1**, with exception of an additional methoxy group due to the presence of a methyl signal at δ_H 3.48 (3H, s) and δ_C 54.3 (q). This substituent was deduced to replace the hydroxy group at C-22 of **1** on the basis of HMBC correlations between the methoxy protons and C-22 (δ_C 84.0, d), and in turn between H-22 (δ_H 4.88, d, *J*=5.5 Hz) and C-24 (δ_C 74.0, s), C-28 (δ_C 135.8, s), C-29 (δ_C 132.6, s) and C-20 (δ_C 114.5, d). Accordingly, the structure of **2** was identified to be 22-methoxy-shearinine A.

Table 1. ^{13}C NMR data for shearinine D–K (**1**–**8**)[a] in $CDCl_3$

Position	1	2	3	4	5	6	7	8
2	153.8 s	153.7 s	151.0 s	152.0 s	177.1s	176.8 s	176.9 s	151.4 s
3	51.8 s	51.7 s	51.6 s	51.7 s	57.5 s	57.3 s	57.5 s	51.4 s
4	39.9 s	39.9 s	39.9 s	39.9 s	41.3 s	41.4 s	41.4 s	39.9 s
5	27.0 t	27.0 t	27.0 t	27.1 t	27.3 t	27.3 t	27.3t	26.9 t
6	28.3 t	28.3 t	28.3 t	28.2 t	28.3 t	28.4 t	28.3 t	28.3 t
7	104.4 s	104.3 s	104.4 s	104.3 s	104.0 s	104.0 s	104.0 s	104.4 s
9	88.1 d	88.0 d	88.0 d	88.0 d	87.8 d	87.9 d	87.9 d	87.9 d
10	197.0 s	197.0 s	197.1 s	196.9 s	196.8 s	196.8 s	196.8 s	197.1 s
11	117.8 d	117.7 d	117.6 d	117.8 d	118.2 d	118.3 d	118.2 d	117.6 d
12	169.6 s	169.5 s	169.8 s	169.4 s	169.3 s	169.3 s	169.3 s	169.8 s
13	77.8 s	77.6 s	77.7 s	77.6 s	77.6 s	77.6 s	77.6 s	77.6 s
14	33.8 t	33.9 t	34.0 t	33.9 t	31.8 t	31.7 t	31.8 t	33.9 t
15	21.1 t	21.1 t	21.2 t	21.0 t	25.4 t	25.5 t	25.4 t	21.2 t
16	48.5 d	48.5 d	48.4 d	48.4 d	34.9 d	34.6 d	34.7 d	48.5 d
17	27.5 t	27.6 t	27.7 t	27.5 t	48.5 t	48.3 t	48.3 t	27.6 t
18	117.6 s	117.5 s	117.2 s	121.1 s	203.2 s	203.0 s	202.7 s	116.9 s
19	126.9 s	126.8 s	123.0 s	124.1 s	130.3 s	134.2 s	131.6 s	123.6 s
20	113.9 d	114.5 d	113.7 d	115.3 d	124.1 d	125.8 d	129.7 d	118.4 d
21	135.2 s	135.7 s	135.1 s	126.5 s	141.6 s	144.0 s	139.3 s	131.3 s
22	76.4 d	84.0 d	36.2 t	194.2 s	37.1 t	33.1 t	31.0 t	31.8 t
23	60.2 d	53.5 d	143.1 s	136.6 s	150.6 s	48.5 d	121.5 d	123.8 d
24	73.8 s	74.0 s	73.6 s	72.1 s	73.4 s	74.2 s	133.5 s	132.6 s
26	72.4 s	72.5 s	71.4 s	71.0 s	71.4 s	72.6 s	134.3 s	131.9 s
27	120.9 d	120.8 d	34.5 t	34.9 t	34.2 t	126.3 d	121.0 d	124.3 d
28	138.6 s	135.8 s	139.5 s	153.1 s	131.5 s	137.5 s	31.2 t	32.0 t
29	131.8 s	132.6 s	131.8 s	136.9 s	136.6 s	136.2 s	145.4 s	139.0 s
30	102.6 d	102.6 d	101.4 d	103.8 d	116.7 d	118.7 d	127.5 d	111.4 d
31	141.1 s	141.1 s	139.3 s	141.4 s	150.1 s	144.6 s	134.8 s	131.5 s
32	16.2 q	16.2 q	16.1 q	16.3 q	17.5 q	17.5 q	17.4 q	16.2 q
33	23.6 q	23.6 q	23.6 q	23.7 q	24.4 q	24.4 q	24.0 q	23.6 q
34	78.8 s	78.8 s	78.7 s	78.8 s	78.6 s	78.6 s	78.6 s	78.7 s
35	23.0 q	23.1 q	23.1 q	23.1 q	23.0 q	23.1 q	23.0 q	23.1 q
36	28.9 q	28.9 q	28.9 q	28.9 q	29.2 q	28.8 q	28.8 q	28.8 q
37	30.1 q	30.0 q	30.4 q	29.1 q	30.6 q	31.4 q	17.98 q	17.9 q
38	23.0 q	22.8 q	30.4 q	29.1 q	28.8 q	22.4 q	25.77 q	25.7 q
39	29.3 q	29.9 q	29.7 q	29.7 q	29.8 q	29.9 q	17.91 q	17.9 q
40	31.9 q	31.9 q	29.6 q	29.7 q	30.1 q	29.6 q	25.74 q	25.7 q
OCH_3		54.3 q						

[a] Chemical shifts (δ) in ppm.

Table 2. ^{1}H NMR data for shearinine D–K (**1**–**8**)[a] in $CDCl_3$

Position	**1**	**2**	**3**	**4**	**5**	**6**	**7**	**8**
1	7.75 s	7.69 s	7.68 s	7.86 s	7.20 s	7.16 s	7.03 s	7.54 s
5	1.85 m, 2.70 m	1.86 m, 2.72 m	1.80 m, 2.70 m	1.81 m, 2.74 m	1.95 m, 2.88 dd 10.0, 14.5	1.97 m, 2.88 dd 10.3, 14.9	1.95 m, 2.85 dd 10.0, 14.7	1.80 m, 2.68 dd 10.5, 13.9
6	2.08 m, 2.85 m	2.05 m, 2.82 ddd 3.0, 9.7, 12.4	2.01 m, 2.82 ddd 3.1, 10.6, 13.7	2.03 m, 2.83 ddd 3.4, 10.2, 13.6	1.65 m, 2.68 ddd, 2.0, 10.9, 13.3	1.62 m, 2.71 ddd 2.7, 10.0, 13.7	1.64 m, 2.70 ddd 2.9, 10.1, 13.0	2.03 m, 2.80 ddd 3.2, 10.2, 13.4
9	4.33 s	4.34 s	4.34 s	4.34 s	4.29 s	4.31 s	4.31 s	4.33 s
11	5.85 s	5.87 s	5.86 s	5.87 s	5.71 s	5.75 s	5.76 s	5.86 s
14	H_α 1.93 ddd 3.0,3.5,13.5, H_β 2.01 m	1.92 m, 2.02 m	1.93 m, 2.10 m	1.90 m, 2.05 m	1.54 m, 1.93 m	1.55 m, 1.92 m	1.55 m, 1.91 m	1.90 m, 2.06 m
15	H_α 2.07 m, H_β 1.82 m	2.08 m, 1.85 m	2.04 m, 1.80 m	2.08 m, 1.80 m	1.54 m, 1.74 m	1.57 m, 1.78 m	1.50 m, 1.74 m	2.05 m, 1.80 m
16	2.83 m	2.85 m	2.83 m	2.83 m	3.08 m	3.06 m	2.98 m	2.80 m
17	H_α 2.45 dd 10.5, 13.0, H_β 2.75 dd 6.5, 13.0	2.47 dd 10.5, 13.0, 2.76 dd 6.5, 13.0	2.08 m, 2.76 dd 6.3, 12.7	2.42 dd 12.0, 13.5, 2.75 dd 6.5 13.5	3.17 dd 4.0, 17.5, 2.50 dd 3.0, 17.5	3.13 dd 4.0, 17.0, 2.49 dd 2.7, 18.0	3.09 dd 4.1,17.4, 2.45 dd 3.4,17.8	2.41 dd 10.7, 13.0, 2.72 dd 6.3, 13.2
20	7.50 s	7.47 s	7.49 s	7.50 s	7.73 s	7.51 s	7.48 s	7.23 s
22	4.98 d 5.6	4.88 d 5.5	3.38 br s		3.40 br s	3.08 m, 2.63 dd 8.3, 8.6	3.31 d 7.0	3.41 d 6.5
23	2.69 dd 2.8, 5.6	2.92 dd 2.6, 5.5				2.92 dd 2.9, 5.7	5.22 t 6.5	5.32 t 6.5
27	5.98 d 2.8	5.99 d 2.6	2.45 br s	2.42 s	2.38 br s	6.12 d 2.5	5.17 t 7.0	5.32 t 6.5
28							3.29 d 6.5	3.42 d 6.5
30	7.36 s	7.37 s	7.13 s	6.82 s	6.87 s	7.06 s	6.84 s	7.12 s
32	1.41 s	1.42 s	1.38 s	1.39 s	1.69 s	1.69 s	1.68 s	1.36 s
33	1.25 s	1.25 s	1.26 s	1.25 s	1.18 s	1.23 s	1.13 s	1.22 s
35	1.20 s	1.21 s	1.20 s	1.21 s	1.13 s	1.18 s	1.14 s	1.20 s
36	1.46 s	1.47 s	1.47 s	1.46 s	1.43 s	1.44 s	1.44 s	1.45 s
37	1.51 s	1.48 s	1.45 s	1.49 s	1.45 s	1.14 s	1.67 s	1.74 s
38	1.14 s	1.10 s	1.45 s	1.49 s	1.45 s	1.35 s	1.78 s	1.76 s
39	1.36 s	1.37 s	1.35 s	1.37 s	1.30 s	1.33 s	1.72 s	1.74 s
40	1.37 s	1.38 s	1.35 s	1.37 s	1.34 s	1.38 s	1.78 s	1.76 s
OCH_3		3.48 s						

[a] Chemical shifts (δ) in ppm.

Shearinine F (**3**) possessed the same molecular formula as shearinine A, as deduced from HRFABMS ($C_{37}H_{45}NO_5$, *m*/*z* 583.3291, calcd 583.3292). The ^{1}H and ^{13}C NMR data of rings C–I were in close agreement with those of the respective portion in **1**, **2**, and shearinine A. However, the NMR data of **3** revealed the presence of a methylene group [δ_H 2.45 (2H, br s), δ_C 34.5 (t)] and a quaternary olefinic carbon at δ_C 143.1 (s), instead of the C-23 methine group and the C-27 olefinic methine of shearinine A. Thus, the C-27–C-28 double bond of shearinine A was assumed to be relocated between C-23 and C-28 in **3**. The HMBC correlations between H_3-37, H_3-38 (δ_H 1.45, s, 6H), and C-23 (δ_C 143.1) and between H_3-39, H_3-40 (δ_H 1.35, s, 6H), and C-27 (δ_C 34.5, t) supported the new position of the double bond. The structure of **3** was thus determined to be Δ23,26-*iso*-shearinine A.

HRFABMS data of shearinine G (**4**) at *m*/*z* 597.3109 ($C_{37}H_{43}NO_6$, calcd 597.3085) indicated an oxidized derivative of **3**. The ^{1}H and ^{13}C NMR data of **4** were very similar to those of **3**, with the exception of an additional keto carbonyl at δ_C 194.2 (s), which was found instead of the C-22 methylene group of **3** (Table 1). The new keto group was deduced to be located at C-22, as evidenced by an HMBC correlation with H-20 (δ_H 7.50, s). Other HMBC correlations for ring A were consistent with those of **3**. The downfield shift of ^{13}C NMR signals of C-28 and C-29, and the upfield shift of those for C-23 and C-21 supported the location of the new keto group. Therefore, the structure of **4** was determined as 22-*oxo*-shearinine F.

2.2. Stereostructures of shearinines D (1)–G (4)

The good agreement of the respective NMR data of **1** with those of shearinine A,[11] together with NOESY data and proton coupling constants indicated that both compounds shared the same relative configuration of ring fusions. Additionally, the identical relative configuration at rings E–H was shown by NOE correlations between H_3-32 and H-17α (δ_H 2.45, dd, J =10.5, 13.0 Hz) and also between H_3-33 and H-16 (δ_H 2.83, m). A $^3J_{H,H}$ coupling constant of 10.5 Hz pointed to an axial–axial coupling between H-17α and H-16, thus confirming trans fusion of rings E–F and F–G. Furthermore, NOE correlations between H-11 and H-14α and between H_3-33 and H-14β suggested the same α-orientation of the hydroxyl group at C-13 as in shearinine A. For the ring A–B fusions, NOE correlations between H-22 and H_3-38 and between H-23 and H_3-37 implied H-22 and H-23 to be on opposite faces. The ^{1}H and ^{13}C NMR data at C-22 and C-23 of **1** were also in good agreement with those of janthitrem B and E,[14] thus allowing to determine the relative H-22β and H-23α configurations (Fig. 2).

These investigations established the relative configurations in the 'Western' A–B fragment on the one hand and in the 'Eastern' E–I portion on the other, but left the configuration

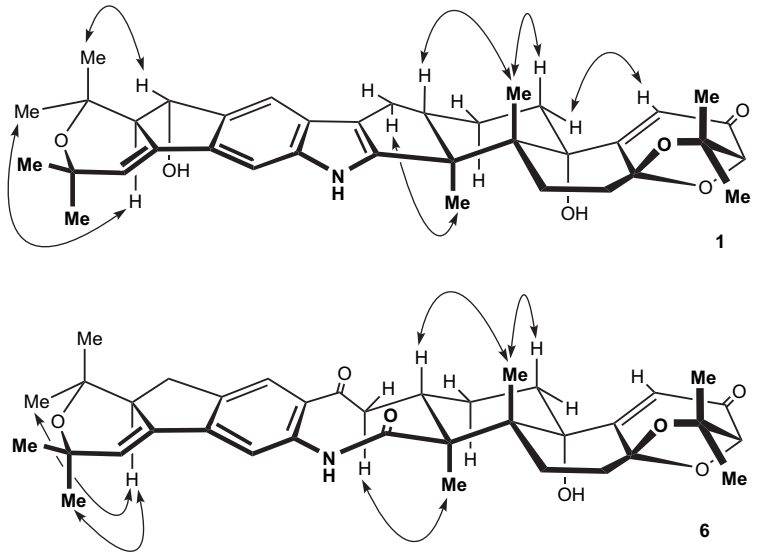

Figure 2. Key NOE correlations of **1** and **6**.

of the two portions relative to each other and the absolute configuration of the entire molecule open. Shearinine D (**1**) shares a partially identical moiety of rings E–G with paspaline (**11**), which on the basis of biosynthetic reasoning is supposed to be of identical absolute configuration. The absolute configuration of **11** was assumed from an X-ray structure analysis[15] and latter confirmed by total synthesis.[16] On the basis of optical rotation values the paspaline of the present study was determined to be of identical configuration as the known one [paspaline (**11**): $C_{28}H_{39}NO_2$, $[\alpha]_D$ −14 versus −23 in Ref. 17]. If this assumption was correct, only two remaining stereoisomeric structures should be possible for shearinine D, viz. the two diastereomers with (3*S*,4*R*,7*S*,9*R*,13*S*,16*S*,22*S*,23*R*)-configuration (**1a**) and with (3*S*,4*R*,7*S*,9*R*,13*S*,16*S*,22*R*,23*S*) (**1b**), i.e., both of them with the same configuration in the 'Eastern' E–I portion as paspaline (for rings E–G), while the 'Western' A–B part could exist in both possible enantiomorphous versions.

Since no crystals were available suited for an X-ray structural analysis, quantum chemical circular dichroism (CD) calculations[18,19] were performed. Starting the calculations at the semiempirical PM3 level, five minimum structures were obtained each for **1a** and **1b**.[20] The single CD spectra of these structures obtained from OM2 single excited states calculations were then in each case added following the Boltzmann statistics and the two overall CD spectra thus obtained were submitted to a UV correction[18] and then compared with the experimental one. This comparison revealed a quite good agreement between the calculated spectrum of **1a** and the measured CD curve (Fig. 3, left), whereas the predicted CD spectrum of its enantiomer, *ent*-**1a** (not shown)

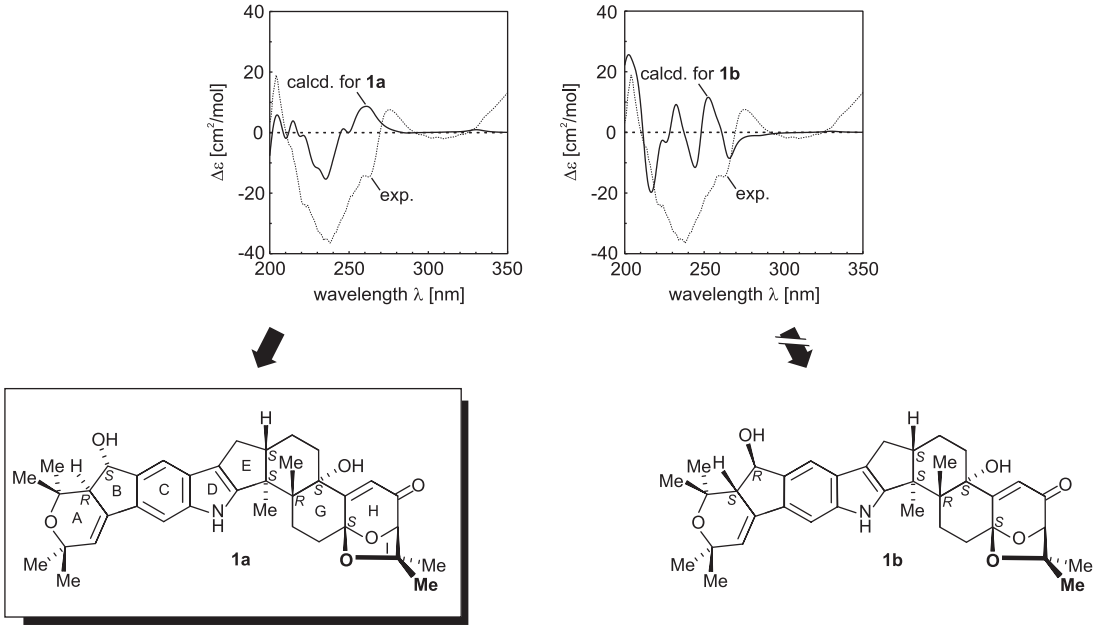

Figure 3. Assignment of the absolute configuration of **1** by comparison of the calculated CD spectra of its diastereomers, **1a** and **1b**, with the experimental curve.

was fully opposite. But also the spectrum calculated for **1b** (Fig. 3, right), although giving a qualitatively worse agreement with the experimental curve than that of **1a**, still corresponded better to the experimental one than the one calculated for *ent*-**1b** (not shown), clearly indicating that indeed the 'Eastern' part of the molecule, i.e., the ring E–I sequences are, as assumed above, configured like in rings E–G of paspaline (as also indicated for the two possible diastereomers in Fig. 3). The fact that the spectrum calculated for **1a** is qualitatively much better than the one predicted for **1b** furthermore suggested that the previous diastereomer, **1a**, corresponds to the natural product.

To investigate this at a higher computational level, DFT calculations were performed, this time resulting in only two minimum structures for each diastereomer. Surprisingly, these higher-level and more demanding TD DFT calculations did not show any major improvements (not shown) as compared to those obtained at the semiempirical level. Nonetheless, the TD DFT calculations likewise confirm that the absolute configuration at the stereogenic centers of the rings E–G are identical to those of paspaline (**11**), likewise corroborating the absolute configuration at rings H and I. Moreover, together with the semiempirical results shown in Figure 3, an assignment of the western portion is possible, too (see above). Thus, the conclusion can be drawn that natural shearinine D possesses the stereostructure **1a**, i.e., with (3*S*,4*R*,7*S*,9*R*,13*S*,16*S*,22*S*,23*R*)-configuration.

The stereostructure of rings E–I of shearinines E (**2**), F (**3**), and G (**4**) was assumed to be identical to that of **1** according to very similar ^{1}H, ^{13}C and NOE NMR data and biosynthetic reasoning. For confirming the configuration of the ring A–B junctions in **2** to be identical to **1**, NOE correlations were observed between H-23 (δ_H 2.92, dd) and the methoxy protons and H_3-37 (δ_H 1.48, s), and between H-22 and H_3-38 (δ_H 1.10, s) as well as similar proton coupling constants of H-22. Due to biosynthetic reasoning, we assume compounds **1**–**4** to have identical absolute configuration.

2.3. Structures of shearinines H (5)–K (8)

The molecular formula of shearinine H (**5**) was determined as $C_{37}H_{45}NO_7$ by HRESIMS (616.3275 $[M+H]^+$, calcd 616.3269) and was in accordance with NMR results. ^{13}C NMR data indicated the presence of three carbonyl carbons at δ_C 196.8 (s), 203.2 (s), and 177.1 (s). The latter was suggested to be an amide because of HMBC correlation of this carbon signal with a D_2O exchangeable proton at δ_H 7.20 (s). Comparison of the NMR data of **5** with those of shearinine C ($C_{37}H_{47}NO_7$) revealed that both compounds shared the same basic skeleton with a central eight-membered keto-amide ring.[11] Differences between the two compounds were found in rings A and H. A C-23–C-28 double bond as in **3** and **4** was proposed for **5** on the basis of the similarity of the corresponding ^{1}H, ^{13}C NMR data and HMBC correlations. Likewise, ring H in compound **5** was suggested to carry the identical 1,3-dioxolane unit as found for co-metabolites **1**–**4**. The stereostructure of **5** was deduced to be identical to that of **3**, due to similar NOESY correlations for rings E–H. Moreover, this became obvious when **5** was identified as a product of autoxidation of **3** when left in chloroform during NMR measurements (50% conversion in 24 h).

Shearinine I (**6**) showed the same molecular formula as that of **5** by HRFABMS data. The ^{1}H, ^{13}C and HMBC NMR data of **6** differed from those of **5** solely for ring A, by indicating a substitution pattern identical to that of compounds **1** and **2**. This was deduced by the presence of an olefinic (δ_H 6.12, d, J=2.5 Hz, H-27; δ_C 126.3, d, C-27) and an aliphatic methine (δ_H 2.92 dd, J=2.9, 5.7 Hz, H-23; δ_C 48.5, d, C-23) and HMBC correlations between C-27 and H_3-39 (δ_H 1.33, s) and H_3-40 (δ_H 1.38, s), and between C-23 and H_3-37 (δ_H 1.14, s) and H_3-38 (δ_H 1.35, s). The relative configuration of **6** was identified to be the same as that of **5** for rings F–I and is in agreement with that of **1** and **2** for rings A–B according to the close similarity of NMR and NOE data and biosynthetic reasoning.

The molecular formula of shearinine J (**7**) was determined to be $C_{37}H_{47}NO_6$ by HRESIMS (*m*/*z* 624.3291 $[M+Na]^+$, calcd 624.3296), indicating 15° of unsaturation. Comparison of ^{1}H and ^{13}C NMR data, as well as 2D NMR data (COSY, HMQC, HMBC, and NOESY) revealed the partial structure of rings F–I to be identical to that in **5** and **6**. The remaining ^{1}H NMR signals for four methyl singlets at δ_H 1.67 (s, H_3-37), 1.78 (s, H_3-38), 1.72 (s, H_3-39), and 1.78 (s, H_3-40), two vinylic protons at δ_H 5.22 (t, J=6.5 Hz, H-23), 5.17 (t, J=7.0 Hz, H-27), and two methylene protons at δ_H 3.31 (d, J=7.0 Hz, H_2-22) and 3.29 (d, J=6.5 Hz, H_2-28) were attributable to two isoprene units, which was confirmed by HMBC data. The two isoprene moieties were determined to be located at C-21 and C-29 of the aromatic ring because of the two aromatic protons, H-20 and H-30, appeared as singlets and they showed HMBC correlations with the respective methylene carbons of the two side chains, such as δ_H 6.84 (s, H-30) correlating to δ_C 31.2 (t, C-28) and δ_H 7.48 (s, H-20) correlating to δ_C 31.0 (t, C-22).

HRFABMS data of shearinine K (**8**) (*m*/*z* 569.3515, calcd for $C_{37}H_{47}NO_4$, 569.3499) indicated a deoxygenated derivative of **7**. The ^{1}H and ^{13}C NMR data were in good agreement with those of rings C–I in compounds **1**–**4**. The remaining NMR signals were unambiguously attributed to two isoprene units substituted at C-21 and C-29 like in compound **7**. Compound **8** was partly converted to **7** by autoxidation when left in $CDCl_3$. The relative configuration of **8** was suggested to be identical to that of **1**–**7** according to similar NMR data and NOE correlations.

2.4. BK_{Ca} channel inhibition

Since several related indole alkaloids have been found to be potent inhibitors of calcium-activated potassium channels,[21–23] shearinines D (**1**)–K (**8**) were subjected to electrophysiological experiments on large-conductance calcium- and voltage-activated potassium (BK_{Ca}) channels. Ensemble currents of more than 1000 BK_{Ca} channels present in excised membrane patches of *hSlo1* transfected HEK 293 cells were evoked by repetitive voltage-ramps (up to +150 mV) in a bath solution containing 3 μM free Ca^{2+}. Test substances (100 nM) were applied directly to the cytosolic face of the membrane patch. As shown in Figure 4A, penitrem A as a positive control strongly inhibited BK_{Ca} channels,[21] whereas **1** led to partial inhibition, and block by **3** was negligible. Compounds **1**, **2**, **4**, and **8** caused current reduction greater than 30%. Compared to penitrem A, the

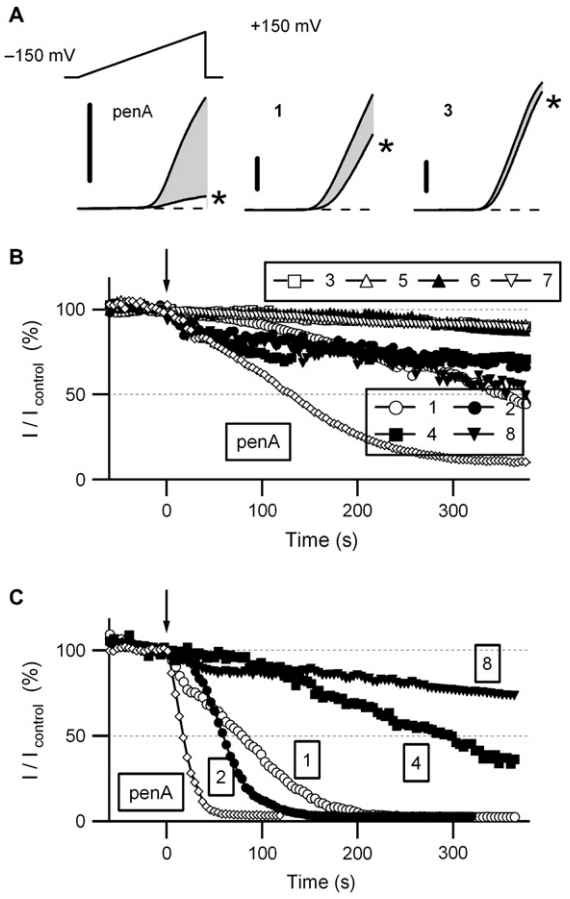

Figure 4. BK_{Ca} channel inhibition. (A) Representative BK_{Ca} currents, elicited by voltage-ramps (top left) before and 4 min after (*) addition of 100 nM of the compound indicated. The shaded areas highlight the current fractions blocked. Scale bars: 15 nA. (B, C) Time course of normalized maximal currents, for 100 nM (B) and 1 μM (C) test compound. Arrows indicate the start of compound application.

onset of block was slower and the overall efficacy was reduced. Compounds **3**, **5**, **6**, and **7** exhibited only negligible effects, reducing BK_{Ca} currents by less than 10%. Figure 4B summarizes the time course of BK_{Ca} inhibition by shearinines D (**1**)–K (**8**). It should be noted that only inhibition by **1** (and penitrem A) was statistically significant different when pairwise compared to 'non-blocking' compounds (**3**, **5**, **6**, and **7**). Therefore, the inhibitory effects of **1**, **2**, **4**, and **8** were reassessed at 10-fold higher concentrations. As depicted in Figure 4C, the effectiveness of BK_{Ca} inhibition of **1**, **2**, and (although less pronounced) **4** was increased at 1 μM (compared to 100 nM) and the onset was accelerated. By contrast, the effects of **8** did not resemble typical channel inhibition, since they did not increase with concentration. As estimated from their blocking efficacies at 0.1 and 1 μM, IC_{50} values for **1** and **2** were 150 nM and 170 nM, respectively, i.e., ca. 10-fold higher than for penitrem A (17 nM).

3. Discussion

The indole alkaloids of the janthitrem class and related compounds are a small group of about 50 metabolites with a unique polycyclic skeleton and are mainly produced by fungi of the genera *Penicillium*, *Aspergillus*, and *Claviceps*.[24] The newly found shearinines D (**1**)–K (**8**) carry some structural features that were not known within this class of compounds before. This includes the localization of a double bond at C-23–C-28, as in **3**–**5**, instead of one at C-27–C-28 and the appearance of a keto group at C-22. The only other indole alkaloids that carry two 3-methyl-2-butenyl chains in *ortho* position as in **7** and **8**, are cristatin A, cryptoechinulin G, and nodulisporic acid E.[24]

Based on increasing structural complexity, the compounds identified in this study can be fitted into a hypothetical biosynthetic grid that provides insights into the biosynthesis of the shearinine/paspalitrem-type janthitrem indole alkaloids (Scheme 1). The earliest known intermediate is suggested to be paspaline (**11**). The initial elongation by two dimethylallyl pyrophosphate units on the aromatic ring is suggested to occur by intermediate cyclization of ring I as witnessed by the occurrence of paspalitrem A (**10**). After the bis-prenylation, shearinine K (**8**) might be oxidatively cyclized to produce rings A–B of shearinine A (**9**). This intermediate corresponds to the missing link that was proposed for the biosynthetic grid of the nodulosporic acids.[25] From **9**, the enzymatic biosynthesis is suggested to proceed either by oxidation at C-22 toward compound **1** and its methoxy derivative **2** or by olefinic rearrangement toward **3**. The latter intermediate could be further oxidized to the highly stabilized keto-analogue **4**. Considering the modifications at ring B, a reverse procedure by reduction at C-22 was suggested for the formation of janthitrem G from janthitrem F.[26] Shearinines H–J (**5**–**7**) are most likely formed by oxidation of the respective intermediates by cleavage of the C-2–C-18 bond. The conversion of **3** to **5** and of **8** to **7** could be readily observed by leaving the respective starting material in chloroform solution (during NMR measurement; approx. 50% conversion during 24 h). Therefore, we suggest an autoxidative process that does not involve biosynthetic enzymes.[27] Interestingly, compounds **1**, **2**, and **4** that are oxidized at C-22 are not susceptible to this reaction. As judged by the overall similar isolated yields of the compounds (3–10 mg), there does not seem to be a major biosynthetic path and the end-products are not favored over the putative intermediates.

Several janthitrem indole alkaloids including paxilline and penitrem A (10 nM) have been shown to inhibit BK_{Ca} channels almost completely.[21] In our hands, penitrem A exhibited slightly weaker but still strong BK_{Ca} inhibition, with an IC_{50} of 17 nM. In line with the observation by McMillan et al. of a similar IC_{50} value for BK_{Ca} inhibition by paxilline,[23] we assume that the quantitative discrepancies arose from differences in the experimental setup (type of channel, recording mode, etc.). In any case, we could clearly show that the two novel shearinines D and E (**1** and **2**), but not the closely related shearinines A (**9**, data not shown) and F (**3**), differing only in the substitution of C-22, have similar BK_{Ca} blocking ability, albeit with lower potency. Thus, shearinines D (**1**) and E (**2**) represent two novel mycotoxins with BK_{Ca} blocking ability in the nanomolar range. Although **4** also exhibited slight BK_{Ca} inhibiting activity, this compound was considered unspecific with respect to its low potency ($IC_{50}>1$ μM), similar e.g. to paspaline.[23] Thus, our data clearly show that the substituents of C-22, similar to those of C-13,[23] are important determinants for BK_{Ca} inhibition by janthitrems.

Future studies have to fully elucidate the structure–activity relationship for BK_{Ca} inhibition by shearinines. Further, it is of interest whether the channel block is specific for (human) BK_{Ca} and how channel inhibition is mediated. As proposed for other tremorgenic mycotoxins,[21] BK_{Ca} blocking shearinines like **1** and **2** may cross the blood–brain barrier and, thus, could be of therapeutical value for treatment of special forms of epilepsia.[4] Besides, they may be helpful tools to specifically modifying BK_{Ca} calcium- and voltage-dependent gating processes, which are still not fully understood.

4. Experimental section

4.1. General experimental procedures

The UV spectra were recorded on Lengguang 756-MC spectrophotometer. The IR spectra were determined on a Thermo Nicolet Nexus 470 FT-IR spectrometer. CD spectra were measured on a J-715 spectropolarimeter (JASCO, Gross-Umstadt, Germany) at room temperature using a 0.1 cm standard cell and spectro-photometric grade MeOH, and are reported in $\Delta\varepsilon$ values (cm^2/mol) at the given wavelength λ (nm). ^1H NMR and ^{13}C NMR spectra were recorded on AVANCE-500 FT 500 MHz NMR spectrometer using TMS as an internal standard. ESIMS spectra were recorded in the MDS-SCIEX-QSTAR mass spectrometer (ABI, USA). HRFABMS spectra were obtained from Bruker Daltonics APEX-II FT-ICR mass spectrometer. Column chromatography was carried with silica gel (200–300 mesh), and HF-254 silica gel for TLC was provided by Qingdao Marine Chemistry Co. Ltd. Sephadex LH-20 (18–110 μm) was purchased from Pharmacia.

4.2. Computational methods

All structure optimizations were accomplished with the program package Gaussian 03[28] using the PM3[29] Hamiltonian or the hybrid DFT functional B3LYP[30] together with Pople's 6-31G(d).[31] Rotational strengths for the electronic transition from the ground state to the singly excited states were obtained by OM2[32] calculations with MNDO99[33] or by time dependent B3LYP/6-31G(d) calculations considering the first 35 excited states with Gaussian 03. The corresponding values obtained were summed energetically weighted, following the Boltzmann statistics. The overall CD spectra were simulated as sums of Gaussian functions centered at the wavelengths of the respective electronic transitions and multiplied by the corresponding rotational strengths and transformed into $\Delta\varepsilon$ values. Finally, the obtained CD spectra were UV-corrected.[18]

4.3. Mangrove plant material

The specimen of *A. corniculatum* (Aegiceratacеae) was collected near Xiamen City of Fujian Province, People's Republic of China, in August, 2002, and authenticated by Prof. Peng Lin of Xiamen University. The sample (No. 200208082) was deposited in the School of Pharmaceutical Sciences, Peking University. *Penicillium* sp. strain (HKI0459) was isolated from the stems of the plant and was deposited in the strain collection of the Hans-Knöll Institute, Jena, Germany.

4.4. Strain isolation, characterization, and cultivation

The strain was isolated from the mangrove plant *A. corniculatum*. Pieces of the stem were rinsed with sterile water, sterilized by soaking in 70% ethanol (1 min) and 3.5% NaCl solution (3 min), and rinsed again with sterile water. Tiny pieces obtained by cutting with a sterile knife were placed on agar plates with GPY agar, which was supplemented with streptomycin (0.1 g/L) and chloramphenicol (0.2 g/L), and incubated at 22 °C until growth appeared. Fungal colonies were transferred to fresh agar plates for further growth. General laboratory cultivation was performed on malt agar [malt extract 20.0 g/L, yeast extract 2.0 g/L, glucose 10.0 g/L, $(NH_4)_2HPO_4$ 0.5 g/L, pH 6.0] or the respective liquid medium at 22 °C. For long-term preservation, cultures grown on agar plates supplemented with 5% glycerol were maintained in the vapor phase of liquid nitrogen. The fungal isolate has been deposited in the strain collection of the Leibniz Institute for Natural Products Research and Infection Biology. The fungus was taxonomically studied by morphological criteria and was assigned as *Penicillium* sp. belonging to the subgenus *Furcatum* on the basis of macro- and micromorphological criteria. The strain is closely related to *Penicillium janthinellum* and *Penicillium simplicissimum*, but showed clearly distinct features (e.g., red reverse color): It could not be assigned to a species according to the concept of Pitt.[34]

For screening purposes, the strain was grown in 250 mL Erlenmeyer flasks with 100 mL of the production culture medium, consisting of saccharose 20 g/L, soybean flour 10 g/L, cornsteep 10 g/L, and KCl 8 g/L, adjusted to pH 6.5 prior to sterilization. It was inoculated with pieces (1×1 cm^2) from an agar plate of a well grown culture and cultivated as resting culture for 17 days at 22 °C. The production culture was carried out in a 300 L fermentor filled with 200 L of the above production medium; it was grown for 10 days at 22 °C (aeration 50 L/min, pH 6.5) and stirred at 125 rpm. The inoculum (2 L) was obtained after several steps of resting cultures with increasing cultivation volume in a modified malt extract medium [malt extract 10.0 g/L, yeast extract 4.0 g/L, glucose 4.0 g/L, $(NH_4)_2HPO_4$ 0.5 g/L, pH 5.5].

4.5. Extraction and isolation

Fermentation supernatant of *Penicillium* sp. subsp. was filtered by centrifugation. Then the mycelium of the strain (70 g) was extracted by acetone and dried. The extract (5 g) was subjected to a Sephadex LH-20 column and eluted with MeOH to get 12 fractions (F1–F12). Fraction F12 (150 mg), showing positive reaction to Dragendorf and anisaldehyde reagents, was subjected to a silica gel column eluting with a gradient $CHCl_3$–MeOH to yield **1** (10 mg, 10:1) and **9** (3.0 mg, 5:1). The remaining fractions were combined and passed through Sephadex LH-20 column eluting with MeOH–H_2O (9:1) to afford four portions monitored by TLC. P3 and P4 were the subfractions from F12. P4 (30 mg) was purified by semi-preparative HPLC with MeOH–H_2O (4:1) as a mobile phase to yield **5** (5 mg), **4** (3.5 mg), **2** (3.0 mg), and **6** (3.1 mg). P3 (35 mg) was followed by the same way as P4 with MeOH–H_2O (9:1) as a mobile phase to obtain **7** (10 mg), **8** (5.2 mg), **10** (5.0 mg), **11** (7.0 mg), and **3** (3.1 mg).

4.5.1. Shearinine D (1). White amorphous powder; $[\alpha]_D$ +67.7 (*c* 0.3, $CHCl_3$); UV (MeOH) λ_{max} 210, 236, 260, 330 nm; CD (MeOH): $\Delta\varepsilon_{195}$ +1.7, $\Delta\varepsilon_{199}$ −0.4, $\Delta\varepsilon_{204}$ +3.4, $\Delta\varepsilon_{238}$ −6.6, $\Delta\varepsilon_{276}$ +1.4, $\Delta\varepsilon_{309}$ −0.4, $\Delta\varepsilon_{354}$ +2.7; IR (KBr) ν_{max} 3421, 2974, 2933, 1685, 1621, 1515, 1455, 1364, 1270, 1220, 1158, 1140, 1048, 1006, 973, 910 cm^{-1}; ^1H and ^{13}C NMR data, see Tables 1 and 2; ESIMS *m/z* 600 $[M+H]^+$, 582 $[M-OH]^+$, 524, 510, 494, 440; HRESIMS *m/z* 622.3163 $[M+Na]^+$ (calcd for $C_{37}H_{45}NO_6Na$, 622.3139).

4.5.2. Shearinine E (2). White amorphous powder; $[\alpha]_D$ +8.9 (*c* 0.2, $CHCl_3$); UV (MeOH) λ_{max} 204, 234, 264, 332 nm; IR (KBr) ν_{max} 3412, 2925, 2854, 1685, 1613, 1457, 1362, 1273, 1223, 1130, 1099, 1049 cm^{-1}; ^1H and ^{13}C NMR data, see Tables 1 and 2; ESIMS *m/z* 612 $[M-H]^-$; HRFABMS *m/z* 613.3396 (calcd for $C_{38}H_{47}NO_6$, 613.3397).

4.5.3. Shearinine F (3). White amorphous powder; $[\alpha]_D$ +26.4 (*c* 0.3, $CHCl_3$); UV (MeOH) λ_{max} 204, 240, 306 nm; IR (KBr) ν_{max} 3422, 2972, 2928, 2854, 1688, 1615, 1457, 1379, 1274, 1162, 1116, 1048 cm^{-1}; ^1H and ^{13}C NMR data, see Tables 1 and 2; ESIMS *m/z* 582 $[M-H]^-$; HRFABMS *m/z*: 583.3291 (calcd for $C_{37}H_{45}NO_5$, 583.3292).

4.5.4. Shearinine G (4). White amorphous powder; $[\alpha]_D$ +35.7 (*c* 0.1, $CHCl_3$); UV (MeOH) λ_{max} 280 nm; IR (KBr) ν_{max} 3432, 2924, 2857, 1684, 1610, 1548, 1530, 1446, 1382, 1162, 1119 cm^{-1}; ^1H and ^{13}C NMR data, see Tables 1 and 2; ESIMS *m/z* 598 $[M+H]^+$, 596 $[M-H]^-$; HRFABMS *m/z*: 597.3109 (calcd for $C_{37}H_{43}NO_6$, 597.3085).

4.5.5. Shearinine H (5). White amorphous powder; $[\alpha]_D$ +20.2 (*c* 0.3, $CHCl_3$); UV (MeOH) λ_{max} 246, 308 nm; IR (KBr) ν_{max} 3421, 2926, 1680, 1614, 1450, 1382, 1160, 1102 cm^{-1}; ^1H and ^{13}C NMR data, see Tables 1 and 2; ESIMS *m/z* 638 $[M+Na]^+$, 616 $[M+H]^+$, 598, 588, 570, 558, 540, 518, 512, 494, 470, 454, 440, 408, 270, 212; HRESIMS *m/z* 616.3275 $[M+H]^+$ (calcd for $C_{37}H_{46}NO_7$, 616.3269).

4.5.6. Shearinine I (6). White amorphous powder; $[\alpha]_D$ +6.5 (*c* 0.3, $CHCl_3$); UV (MeOH) λ_{max} 245 nm; IR (KBr) ν_{max} 3420, 2925, 1685, 1611, 1380, 1196 cm^{-1}; ^1H and ^{13}C NMR data, see Tables 1 and 2; ESIMS *m/z* 616 $[M+H]^+$, 614 $[M-H]^-$; HRFABMS *m/z*: 616.3278 $[M+H]^+$ (calcd for $C_{37}H_{46}NO_7$, 616.3268).

4.5.7. Shearinine J (7). White amorphous powder; $[\alpha]_D$ +48.5 (*c* 0.3, $CHCl_3$); UV (MeOH) λ_{max} 206, 232 nm; IR (KBr) ν_{max} 3431, 2928, 2959, 1687, 1449, 1383, 1275, 1245, 1106, 1048, 913 cm^{-1}; ^1H and ^{13}C NMR data, see Tables 1 and 2; ESIMS *m/z* 602 $[M+H]^+$, 600 $[M-H]^-$, 556, 498, 287, 256; HRESIMS *m/z*: 624.3291 $[M+Na]^+$ (calcd for $C_{37}H_{47}NO_6Na$, 624.3296).

4.5.8. Shearinine K (8). White amorphous powder; $[\alpha]_D$ +26.7 (*c* 0.2, $CHCl_3$); UV (MeOH) λ_{max} 238, 280 nm; IR (KBr) ν_{max} 3451, 3421, 2972, 2928, 2850, 1687, 1450, 1373, 1273, 1221, 1105, 1047 cm^{-1}; ^1H and ^{13}C NMR data, see Tables 1 and 2; ESIMS *m/z* 568 $[M-H]^-$; HRFABMS *m/z*: 569.3515 (calcd for $C_{37}H_{47}NO_4$, 569.3499).

4.6. Electrophysiological assay

Patch-clamp analysis of BK_{Ca} inhibition by the test substances was performed in symmetrical (140 mM) K^+ solutions on inside-out membrane patches from HEK 293 cells transiently expressing *hSlo1* α-subunits. A detailed description of cell culture, transfection, and electrophysiological recordings is given elsewhere.[35] In brief, membrane patches containing >1000 BK_{Ca} channels were excised into a bath solution containing 3 μM free Ca^{2+} and allowed to equilibrate (>4 min). BK_{Ca} currents were evoked with repetitive (0.25 Hz) 150-ms voltage-ramps (–150 to +150 mV). After 2 min, the respective test substance (freshly diluted in bath solution from 10 mM DMSO stock solutions) was applied for at least 4 min directly to the cytosolic face of the patch. Maximal outward current amplitudes were normalized against control amplitude before blocker application and plotted against time. Penitrem A (Alomone, Jerusalem, Israel) served as a positive control. Data are given as mean±SEM from 3 to 7 independent experiments. Statistical significance was considered for $P<0.05$ according to unpaired, two-sided Student's *t*-tests.

Acknowledgements

This work was supported by grants of the Chinese National High-Tech 863 Project (No. 2003AA624030, 2002AA217081), and NSF China (No. 29932030, 30171106), the German Federal Ministry for Education, Research and Technology (BMBF, 0312849A and CHN 02/322), the Deutsche Forschungsgemeinschaft (DFG, HE 2993/6, SPP 1152), and the Fonds der Chemischen Industrie. Excellent collaboration with Guido Fischer (Technical University Aachen) for taxonomical analysis is gratefully acknowledged.

References and notes

1. Miles, D. H.; Kokpol, U.; Chittawong, V.; Tip-Pyang, S.; Tunsuwan, K.; Nguyen, C. *Pure Appl. Chem.* **1998**, *70*, 2113–2122.
2. Manoharachary, C.; Sridhar, K.; Singh, R.; Adholeya, A.; Suryanarayanan, T. S.; Rawat, S.; Johri, B. N. *Curr. Sci.* **2005**, *89*, 58–71.
3. Petrini, O.; Sieber, T. N.; Toti, L.; Viret, O. *Nat. Toxins* **1992**, *1*, 185–196.
4. Ghatta, S.; Nimmagadda, D.; Xu, X.; O'Rourke, S. T. *Pharmacol. Ther.* **2006**, *110*, 103–116.
5. Grabley, S.; Sattler, I. *Modern Methods of Drug Discovery*; Hilgenfeld, R., Hillisch, A., Eds.; Birkhäuser: Basel, 2001; pp 87–107.
6. Guan, S.; Sattler, I.; Lin, W.; Guo, D.; Grabley, S. *J. Nat. Prod.* **2005**, *68*, 1198–2000.
7. Huang, X.; Roemer, E.; Sattler, I.; Moellmann, U.; Christner, A.; Grabley, S. *Angew. Chem.* **2006**, *118*, 3138–3143; *Angew. Chem., Int. Ed.* **2006**, *45*, 3067–3072.
8. Lin, P.; Fu, Q. *Environmental Ecology and Economic Utilization of Mangroves in China*; Higher Education Press: Beijing, 1995; pp 1–95.

9. Xu, M.; Deng, Z.; Li, M.; Fu, H.; Proksch, P.; Lin, W. *J. Nat. Prod.* **2004**, *67*, 762–766.
10. Xu, M.; Cui, J.; Fu, H.; Proksch, P.; Lin, W.; Li, M. *Planta Med.* **2005**, *71*, 944–948.
11. Belofsky, G. N.; Gloer, J. B.; Wicklow, D. T.; Dowd, P. F. *Tetrahedron* **1995**, *51*, 3959–3968.
12. Cole, R. J.; Dorner, J. W.; Lansden, J. A.; Cox, R. H.; Pape, C.; Cunfer, B.; Nicholson, S. S.; Bedell, D. M. *J. Agric. Food Chem.* **1977**, *25*, 1197–1201.
13. Munday-Finch, S. C.; Wilkins, A. L.; Miles, C. O. *Phytochemistry* **1996**, *41*, 327–332.
14. Wilkins, A. L.; Miles, C. O.; Ede, R. M.; Gallagher, R. T.; Munday, S. C. *J. Agric. Food Chem.* **1992**, *40*, 1307–1309.
15. Fehr, T.; Acklin, W. *Helv. Chim. Acta* **1966**, *49*, 1907–1920.
16. Smith, A. B., III; Mewshaw, R. *J. Am. Chem. Soc.* **1985**, *107*, 1769–1771.
17. Springer, J. P.; Clardy, J. *Tetrahedron Lett.* **1980**, *21*, 231–234.
18. Bringmann, G.; Busemann, S. *Natural Product Analysis*; Schreier, P., Herderich, M., Humpf, H.-U., Schwab, W., Eds.; Vieweg: Wiesbaden, 1998; pp 195–211.
19. (a) Bringmann, G.; Mühlbacher, J.; Reichert, M.; Dreyer, M.; Kolz, J.; Speicher, A. *J. Am. Chem. Soc.* **2004**, *126*, 9283–9290; (b) Bringmann, G.; Rüdenauer, S.; Götz, D. C. G.; Gulder, T. A. M.; Reichert, M. *Org. Lett.* **2006**, *8*, 4743–4746; (c) Bringmann, G.; Gulder, T.; Reichert, M.; Meyer, F. *Org. Lett.* **2006**, *8*, 1037–1040.
20. The CD spectra of those structures that lie energetically higher than 3 kcal/mol above the energetically lowest structure were found not to contribute to the overall CD curve obtained by superposition of the Boltzmann-weighted single spectra.
21. Knaus, H. G.; McManus, O. B.; Lee, S. H.; Schmalhofer, W. A.; Garcia-Calvo, M.; Helms, L. M.; Sanchez, M.; Giangiacomo, K.; Reuben, J. P.; Smith, A. B., III; Kaczorowski, G. J.; Garcia, M. L. *Biochemistry* **1994**, *33*, 5819–5828.
22. DeFarias, F. P.; Carvalho, M. F.; Lee, S. H.; Kaczorowski, G. J.; Suarez-Kurtz, G. *Eur. J. Pharmacol.* **1996**, *314*, 123–128.
23. McMillan, L. K.; Carr, R. L.; Young, C. A.; Astin, J. W.; Lowe, R. G.; Parker, E. J.; Jameson, G. B.; Finch, S. C.; Miles, C. O.; McManus, O. B.; Schmalhofer, W. A.; Garcia, M. L.; Kaczorowski, G. J.; Goetz, M.; Tkacz, J. S.; Scott, B. *Mol. Genet. Genomics* **2003**, *270*, 9–23.
24. *Dictionary of Natural Products on CD Rom*; Hampden Data Services Ltd.: London, 2006.
25. Singh, S. B.; Ondeyka, J. G.; Jayasuriya, H.; Zink, D. L.; Ha, S. N.; Dahl-Roshak, A.; Greene, J.; Kim, J. A.; Smith, M. M.; Shoop, W.; Tkacz, J. S. *J. Nat. Prod.* **2004**, *67*, 1496–1506.
26. Penn, J.; Swift, R.; Wigley, L. J.; Mantle, P. G.; Bilton, J. N.; Sheppard, R. N. *Phytochemistry* **1993**, *32*, 1431–1434.
27. Laakso, J. A.; Gloer, J. B. *J. Org. Chem.* **1992**, *57*, 2066–2071.
28. Frisch, M. J.; Trucks, G. W.; Schlegel, H. B.; Scuseria, G. E.; Robb, M. A.; Cheeseman, J. R.; Montgomery, J. A., Jr.; Vreven, T.; Kudin, K. N.; Burant, J. C.; Millam, J. M.; Iyengar, S. S.; Tomasi, J.; Barone, V.; Mennucci, B.; Cossi, M.; Scalmani, G.; Rega, N.; Petersson, G. A.; Nakatsuji, H.; Hada, M.; Ehara, M.; Toyota, K.; Fukuda, R.; Hasegawa, J.; Ishida, M.; Nakajima, T.; Honda, Y.; Kitao, O.; Nakai, H.; Klene, M.; Li, X.; Knox, J. E.; Hratchian, H. P.; Cross, J. B.; Bakken, V.; Adamo, C.; Jaramillo, J.; Gomperts, R.; Stratmann, R. E.; Yazyev, O.; Austin, A. J.; Cammi, R.; Pomelli, C.; Ochterski, J. W.; Ayala, P. Y.; Morokuma, K.; Voth, G. A.; Salvador, P.; Dannenberg, J. J.; Zakrzewski, V. G.; Dapprich, S.; Daniels, A. D.; Strain, M. C.; Farkas, O.; Malick, D. K.; Rabuck, A. D.; Raghavachari, K.; Foresman, J. B.; Ortiz, J. V.; Cui, Q.; Baboul, A. G.; Clifford, S.; Cioslowski, J.; Stefanov, B. B.; Liu, G.; Liashenko, A.; Piskorz, P.; Komaromi, I.; Martin, R. L.; Fox, D. J.; Keith, T.; Al-Laham, M. A.; Peng, C. Y.; Nanayakkara, A.; Challacombe, M.; Gill, P. M. W.; Johnson, B.; Chen, W.; Wong, M. W.; Gonzalez, C.; Pople, J. A. *Gaussian 03, Revision B.04*; Gaussian, Inc.: Wallingford, CT, 2004.
29. Stewart, J. J. P. *J. Comput. Chem.* **1989**, *10*, 209–220.
30. (a) Lee, C.; Yang, W.; Parr, R. G. *Phys. Rev. B: Condens. Matter* **1988**, *37*, 785–789; (b) Becke, A. D. *J. Chem. Phys.* **1993**, *98*, 5648–5652.
31. (a) Hariharan, P. C.; Pople, J. A. *Theor. Chim. Acta* **1973**, *28*, 213–222; (b) Francl, M. M.; Petro, W. J.; Hehre, W. J.; Binkley, J. S.; Gordon, M. S.; DeFrees, D. J.; Pople, J. A. *J. Chem. Phys.* **1982**, *77*, 3654–3665.
32. Weber, W.; Thiel, W. *Theor. Chem. Acc.* **2000**, *103*, 495–506.
33. Thiel, W. *MNDO 99, Version 6.0*; Max-Planck-Institut für Kohlenforschung: Germany, 2001.
34. Pitt, J. I. *The Genus Penicillium and its Teleomorphic States Eupenicillium and Talaromyces*; Academic: London, New York, Toronto, Sydney, San Francisco, 1979.
35. Gessner, G.; Schönherr, K.; Soom, M.; Hansel, A.; Asim, M.; Baniahmad, A.; Derst, C.; Hoshi, T.; Heinemann, S. H. *J. Membr. Biol.* **2006**, *208*, 229–240.